

# PERFORMANCE COMPARISONS OF EMITTANCE-EXCHANGER BEAMLINES \*

C.R. Prokop <sup>1</sup>, P. Piot <sup>1,2</sup>, B.E. Carlsten <sup>3</sup>, M. Church <sup>2</sup>

<sup>1</sup> Department of Physics, Northern Illinois University DeKalb, IL 60115, USA

<sup>2</sup> Fermi National Accelerator Laboratory, Batavia, IL 60510, USA

<sup>3</sup> Los Alamos National Laboratory, Los Alamos, NM, 87544 USA

## Abstract

Earlier experiments at Fermilab's A0 Photoinjector Laboratory demonstrated successful transverse-to-longitudinal emittance exchange (EEX) using a transverse-deflecting cavity (TDC) located between two identical doglegs. Such a design has the disadvantage of transversely displacing the beam. An alternative is an EEX beamline designed out of a variable  $R_{56}$  bunch compressor chicane. In this paper, we present designs and simulation comparisons for several emittance-exchanger beamlines, including the double-dogleg and chicane designs, as well as variations of the chicane design that allow for increasing its dispersion which proportionally decreases the field-strength requirements on the TDC. These comparisons are performed with PIC models of space charge and coherent synchrotron radiation.

## INTRODUCTION

Transverse-to-longitudinal “emittance exchangers” (EEXs) allow for the exchange of a particle beam’s transverse and longitudinal phase spaces. An early emittance exchanger design consisting of a transverse deflecting cavity (TDC) between two identical doglegs, each comprised of two opposite dipoles and a drift, was demonstrated at Fermilab’s A0 Photoinjector Laboratory [3, 4]. A major disadvantage of such a configuration is its resulting offset of the beam’s direction, which has significant impact on linac design as an elaborate dispersion correction scheme would be needed to operate the beamline in its non emittance-exchanging configuration.

A modification of the original design, based on a variable- $R_{65}$  chicane, allows for the exiting beam to remain in-line with the incoming beam [5]. Furthermore, this design allows for almost-arbitrary adjustment of the dispersion at the TDC location, which reduces its power requirements. In this paper, we present three phase-space exchanger designs and performance comparisons between them.

We use two sets of beam parameters for these studies. The first is based on a study of partially compressed beams at ASTA [6], while the other is a smaller set of emittances used for comparisons with reduced second-order effects. Both are presented in Table 1.

Table 1: Initial beam parameters.

Parameter	symbol	Value (case 1)	Value (case 2)	Units
hor. emittance	$\varepsilon_{x,0}$	10.0	1.0	$\mu\text{m}$
vert. emittance	$\varepsilon_{y,0}$	10.0	1.0	$\mu\text{m}$
long. emittance	$\varepsilon_{z,0}$	39.1	10.0	$\mu\text{m}$
bunch length	$\sigma_{z,0}$	0.8	0.4	mm
LPS chirp	$\mathcal{C}_{z,0}$	0.0	0.0	$\text{m}^{-1}$

## OVERVIEW OF PHASE SPACE EXCHANGER DESIGNS

In this Section we summarize the properties of the three beamlines considered through out this paper. Each of the designs must generally satisfy three different requirements [7]. For the dispersive section upstream of the TDC,  $M_-$ , we must control of the upstream dispersive section’s  $x$  dispersion,  $\eta_-$ , and its derivative,  $\eta_-'$ . For TDC section,  $M_{TDC}$ , we must control the strength of the TDC as  $\kappa = -\frac{1}{\eta_-}$ , operated at zero-crossing. For the downstream section,  $M_+$ , the dispersive section’s transfer matrix must be finely controlled such that the properties satisfy

$$\mathbf{D}_+ = \begin{pmatrix} R_{11,+} & R_{12,+} \\ R_{21,+} & R_{22,+} \end{pmatrix} \mathbf{D}_-, \text{ and} \quad (1)$$

$$\kappa = -1/\eta_-. \quad (2)$$

where the + and – signs refer to values associated to respectively the downstream and upstream dispersive sections and  $\tilde{\mathbf{D}} \equiv (\eta, \eta' \equiv d\eta/ds)$  is the dispersion vector.

The most basic design is the Double Dogleg EEX (DDEEX), of a design similar to that implemented at A0. The dispersion  $\eta$  of each dogleg is 0.5 m, and the TDC is centered between the upstream and downstream doglegs. An accelerating-mode cavity is placed immediately downstream of the TDC to correct for the  $R_{65}$  term [8]. The dipoles are rectangular, and the exact lengths and distances are described in Fig. 1.

A similar design is a the Nominal-Dispersion EEX (NDEEX), in which the bend angles and geometry of each dogleg are the same, except the bend angles of one of them are reversed such that it forms a chicane rather than a pair of symmetric doglegs. Quadrupoles are placed inside the

\* Work supported by LDRD project #20110067DR and by the U.S. DoE Contract No. DE-FG02-08ER41532 with NIU and No. DE-AC02-07CH11359 with Fermilab.

chicane between each of the existing elements, which allow for specific tailoring of the transfer matrix of the upstream and downstream doglegs. The quadrupole magnets are used to adjust the sign of the dispersion the upstream dogleg, while those of the downstream dogleg are used to meet the new requirements on the transfer matrix. For the simplest case, we choose the new dispersion of the upstream dogleg,  $M_-$ , to have the same magnitude as that of the DDEEX, i.e.  $\eta_- = -0.5$ . Diagrams of the DDEEX and NDEEX designs are presented in Fig. 1.

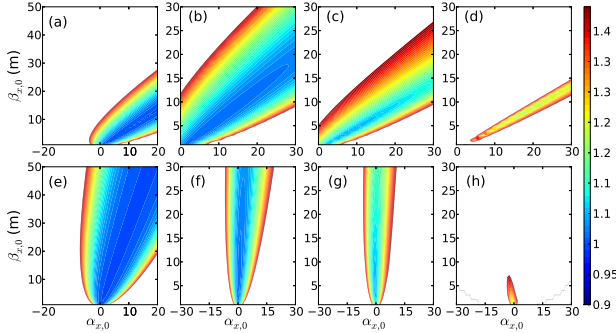


Figure 1: The DDEEX (top) and chicane-like (bottom) emittance-exchanger configurations. The TDC is centered between B2 and B3, and an accelerating mode cavity is placed immediately downstream.

The boosted-dispersion EEX (BDEEX) uses the same components and configuration of the NDEEX chicane. Rather than using the quadrupole magnets in  $M_-$  to change only the sign of its dispersion, we increase its magnitude as well, while correspondingly adjusting the downstream transfer matrix. This has the crucial advantage of decreasing the requirement on the cavity kick-strength, as per Eq. 2. As the dispersion  $\eta_-$  increases, the requirements on  $\eta_+$  become more difficult to satisfy while keeping the beam envelope well-constrained. We explore boosted values of  $2\eta_-$  to  $6\eta_-$ .

Table 2: Beamline parameters of the EEX configurations in Fig. 1

Parameters	Value	Units
Dipole Length	0.30	m
Bend Angle	$\pm 18$	degrees
Beam Energy	50	MeV
$ \eta_- $	[0.5, 1.0, 1.5, 2.0, 2.5, 3.0]	m
$ \eta'_- $	0.0	m
$ \kappa $	[ 2.0, 1.1, 0.66, 0.5, 0.4, 0.33]	$m^{-1}$

The exchanger beamlines were optimized in the simulation code ELEGANT [9], and then imported into IMPACT-Z [10], which allows for the implementation of SC effects with a three-dimensional PIC model, and with a one-dimensional model of CSR [11].

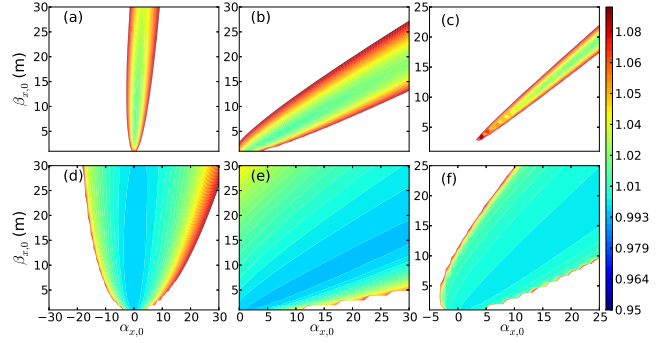


Figure 2: Contour plots comparison of three models (DDEEX (a,d), NDEEX (b,e), and BDEEX(c,f)) with IMPACT-Z for 0 nC for both  $\mathcal{F}_{x \rightarrow z}$  (a-c) and  $\mathcal{F}_{z \rightarrow x}$  (d-f), as functions of the C-S parameters at the EEX entrance,  $\beta_{x,0}$  and  $\alpha_{x,0}$ .

## BEAMLINE COMPARISONS

As a way to measure the relative performance of the various configurations, we performed scans of the initial Courant-Snyder (C-S) parameters,  $\beta_{x,0}$  and  $\alpha_{x,0}$  at the entrance of the EEX. This is required to account for varying optics between each of the configurations and the second-order effects of varying strengths that result from the differing optics.

We compare the core emittance exchanger designs for equivalent doglegs with dispersion of  $|\eta_x| = 0.5\text{m}$ , and the BDEEX design for  $|\eta_x| = 1.0\text{m}$ . Units for the color scales are  $\mu\text{m}$  when presenting the normalized emittances, mm for RMS bunch sizes, and unit-less when presenting the “exchange quality”,  $\mathcal{F}_{x \rightarrow z} \equiv \frac{\varepsilon_{z,f}}{\varepsilon_{x,0}}$  and  $\mathcal{F}_{z \rightarrow x} \equiv \frac{\varepsilon_{x,f}}{\varepsilon_{z,0}}$ , where perfect emittance exchange occurs at  $\mathcal{F} = 1$ . We also define the term “acceptance” with regards to the range over which the emittance exchange quality is near unity.

In Fig. 2, the DDEEX, NDEEX, and BDEEX are compared for the case of no collective effects. Boosting the dispersion causes a notable decrease in the acceptance of initial C-S parameters, as the quadrupole settings within the chicane cause the transverse beam sizes to be more erratic along the beamline.

When SC+CSR are introduced for a 1 nC bunch, as shown in Fig. 3, the acceptance is reduced for all three configurations. Comparisons of  $\sigma_z$  to the contour plots for the emittance exchange quality reveal a significant degradation to the emittance exchange quality that occurs when the beam size is at its minimum, i.e. when the final LPS is upright, a vital part of achieving optimal beam shaping.

This indicates a significant barrier to achieving optimal shaping while also achieving optimal emittance exchange, and that there is some significant trade-off that must be determined when setting the EEX settings.

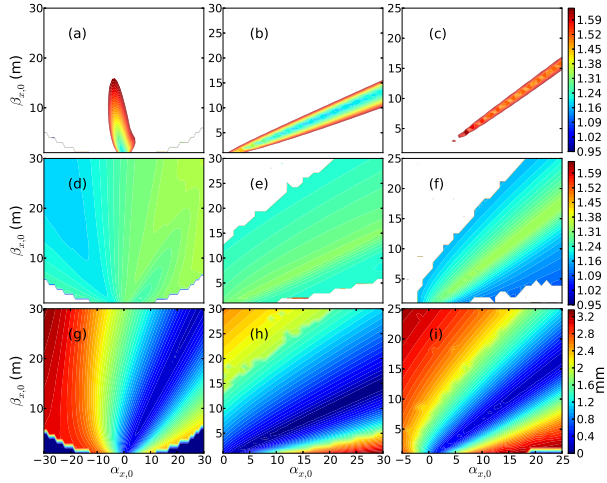


Figure 3: Contour plots comparison of three models (DDEEX, NDEEX, and BDEEX(2 $\times$ ) with IMPACT-Z for 0 nC for both  $\mathcal{F}_{x \rightarrow z}$  and  $\mathcal{F}_{z \rightarrow x}$ , as functions of the C-S parameters at the EEX entrance,  $\beta_{x,0}$  and  $\alpha_{x,0}$ .

## DISPERSION BOOSTING

Boosting the dispersion up to 6x of the nominal value (in this case, 3.0 m) introduces significant complications to beam control. As the  $x$  transfer matrix in the second dog-leg must be controlled to specifically satisfy the basic requirements for perfect emittance exchange, the  $y$  dynamics becomes difficult to control. For an example of optimized functions (via the same method of C-S scans presented earlier), see Fig. 4, using both ASTA and A0-style beam emittances.

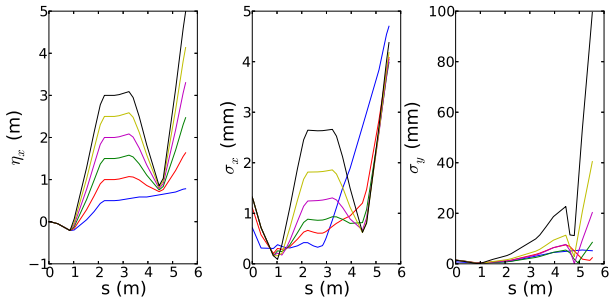


Figure 4: Horizontal dispersion  $\eta_x$  (left),  $\sigma_x$  (middle), and  $\sigma_y$  (right) along the NDEEX and BDEEX designs for  $\eta_- = 0.5$  m (blue), 1.0 m (red), 1.5 m (green), 2.0 m (magenta), 2.5 m (yellow) and 3.0 m (black).

The key difference between these simulations and those of the nominal-dispersion and double-boosted-dispersion is that  $\sigma_y$  is large and divergent, in addition to  $\sigma_x$ , which is large and divergent due to the kick from the TDC. Switching to smaller emittances reduces the beam size and the resultant emittance growth from second-order effects; see Table 3.

The key feature of dispersion boosting is the reduced re-

Table 3: Quality of Emittance Exchange for various dispersions using the BDEEX configuration, along with which emittances were used.

$\eta_-$ (m)	Beam Type	$\mathcal{F}_{x \rightarrow z}$	$\mathcal{F}_{z \rightarrow x}$
0.5	1	1.00	1.00
0.5	2	1.00	1.00
1.0	1	1.04	1.02
1.0	2	1.01	1.00
1.5	1	1.08	1.01
1.5	2	1.01	1.000
2.0	1	2.407	1.05
2.0	2	1.22	1.000
2.5	1	10.42	1.12
2.5	2	3.43	1.01
3.0	1	79.98	1.75
3.0	2	25.35	1.04

quirements on the TDC, so while the quadrupole strengths are increased, the transverse beam size is less dominated by the TDC kick. The trade-offs that must be considered are not simple, and depend greatly on both initial bunch length and transverse emittances. Dispersion-boosting up to 3x of the baseline dispersion is possible with ASTA-scale beam parameters, but greater dispersion is feasible for lower emittance regimes.

## REFERENCES

- [1] P. Emma, et. al, *PRST-AB* **9**, 100702 (2006).
- [2] P.Piot, et. al, *PRST-AB*, **14** 022801 (2011).
- [3] Y.-E. Sun, et. al, *PRL* **105**, 234801 (2010).
- [4] J. Ruan, et. al, *PRL* **106**, 244801 (2011).
- [5] D. Xiang, A. Chao, *Phys. Rev. ST Accel. Beams* **14**, 114001 (2011).
- [6] C. R. Prokop, et. al, *NIM A*, **719**, p. 1728 (2013).
- [7] R. Fliller, Fermilab Report, BeamDocs 2271-v2 (2007).
- [8] A.A. Zholents, M.S. Zolotarev, ANL/APS/LS-327 (2011).
- [9] M. Borland, APS LS-287, September 2000 (unpublished).
- [10] Ji Qiang, et al., *Journal of Comp. Phys.* **163**, p. 434 (2000).
- [11] E.L. Saldin, et. al, *NIM A*, **A 398** p. 373-394 (1997).